# Generalized q-plates and novel vector and vortex beams

Martin Vergara* and Claudio Iemmi
*Facultad de Ciencias Exactas y Naturales, Departamento de Física,*
*Universidad de Buenos Aires, Buenos Aires, Argentina and*
*Consejo Nacional de Investigaciones Científicas y Técnicas, Buenos Aires, Argentina.*
(Dated: October 7, 2019)

We took a generalization of the conventional concept of q-plate, allowing in its definition non linear functions of the azimuthal coordinate, and simulated the resulting fields of applying this kind of element to uniformly polarized input beams, both in the near (Fresnel diffraction) and the far field (Fraunhofer diffraction) approximations. In general terms, when working in the near field regime, the chosen function defines the output polarization structure for linearly polarized input beams, and the phase of the output field for circularly polarized input beams. In the far field regime, it is obtained that when there are non-linearities in the azimuthal variable, the central singularity of the polarization field of a vector or vortex beam may divide into several singularities of lower topological charge, preserving the total charge. Depending on the chosen q-plate function, different particular behaviors on the output beam are observed, which offers a whole range of possibilities for creating novel vector and vortex beams, as well as polarization critical points and singularity distributions.

## I. INTRODUCTION

Vector beams are known for showing a non uniform distribution of the state of polarization (SoP) [1]. The most common beams of this kind are radially and azimuthally polarized beams, particular cases of cylindrical vector beams [2], in which the SoP varies linearly with the azimuthal coordinate $\theta$. Vector beams have been widely studied because of their tight focusing properties [3]. Besides they have potential application to communications [4], optical tweezers and particle micro-manipulation [5–8], material processing [9], quantum entanglement [10] and more.

There are many methods for creating vector beams, generally divided in two categories, active and passive. Active methods consist in modifying the resonant cavity of a laser for obtaining an output vector beam, while passive ones aim to modulate the wave front of a conventional laser beam with suitable optical elements [1]. In the latter case q-plates have become a convenient choice [11].

A conventional q-plate works as a half wave plate in which the director axis rotates as a linear function $q\theta$ of the azimuthal coordinate $\theta$ [12–14]. Its matrix representation in the Jones formalism has the form

$$M_q(\theta) = \begin{pmatrix} \cos(2q\theta) & \sin(2q\theta) \\ \sin(2q\theta) & -\cos(2q\theta) \end{pmatrix}. \qquad (1)$$

When a linearly polarized beam passes through such an element, it becomes a vector beam with a structured polarization pattern in which the azimuth of the polarization ellipses varies as a function $2q\theta$, reaching a total rotation of $4q\pi$. On the other hand, when impinging with a circularly polarized beam, the spin to orbital conversion (STOC) phenomenon takes place: the orbital angular momentum (OAM) of the beam varies according to $\Delta l = \pm 2q$, where the plus sign applies when impinging with left circular polarization and the minus sign when impinging with right circular polarization. In other words, if an uniform left circularly polarized beam (total angular momentum +1) passes through a q-plate, it becomes an uniform right circularly polarized vortex beam with an OAM charge $l = 2q$ (total angular momentum variation of $2(q-1)$). The value $2q$, that gives the times the polarization vector (or phase) completes a $2\pi$ turn along the azimuth coordinate is known as topological charge.

This way, q-plates are high versatile elements, with many potential applications in the field of singular optics, since they allow alternately the creation of phase singularities (vortex beams with OAM) and polarization singularities (vector beams). Additionally, the possibility of using spatial light modulators (SLM), like liquid crystal displays which allow pixel to pixel phase only modulation [15, 16], for the implementation of these devices, gives great flexibility for designing novel vector and vortex beams. It easily allows extending the concept of q-plate, including modulations of the polarization field that are not necessary linear in $\theta$.

Recently there have been advances towards this direction, creating q-plates with different $q$ values depending on the region of the element [17], with non linear functions of $\theta$ for binary codification [18], or with radial dependence for creating high order Laguerre-Gaussian beams [19].

In this paper we simulate an element that rises from generalizing the concept of q-plate, allowing arbitrary (not necessary linear) modulations of the polarization field of a beam, in such a way that we are able to explore complex beams, with novel polarization structures and singularity distributions, and study its propagation properties.

The Jones matrix that describes this generalized q-

* marto@df.uba.ar

plate (Gq-plate) is

$$M_\Phi(\theta) = \begin{pmatrix} \cos(2\Phi(\theta)) & \sin(2\Phi(\theta)) \\ \sin(2\Phi(\theta)) & -\cos(2\Phi(\theta)) \end{pmatrix}, \qquad (2)$$

and it represents a half wave plate in which the director axis angle is an arbitrary function $\Phi(\theta)$. The only requirement we impose is that $\Phi$ is a continuous periodic function in $\theta$, with a period $\tau = 2\pi/n$, being $n$ any integer number.

The potential given by the infinite possible choices of the function $\Phi$ and the flexibility provided by SLMs, makes a significant tool in the field of beam tailoring, allowing further research of new effects and focusing properties of novel kinds of vector and vortex beams. Here we demonstrate the creation of two new type of beams using this technique, for the purpose of illustrating with simple cases the effect of focusing non-linear distributions of polarization and phase, with and without net topological charge.

In section II we simulate Gq-plates with non linear dependence in the azimuthal coordinate, showing its effect on the intensity, phase and polarization distributions of an uniform circular section input beam (top hat beam), for different polarizations. We show the resulting fields both in the near and the far field approximations and give an explanation of these results based on Fourier analysis. We outline in section III a proposal for an experimental implementation using a reflective liquid crystal display (LCoS) with phase-only modulation. The main conclusions are given in section IV.

## II. NON LINEAR GQ-PLATES IN THE AZIMUTHAL VARIABLE

When function $\Phi$ grows non-linearly in the azimuthal coordinate $\theta$, a variety of interesting effects can be observed over the resulting field's amplitude, phase and polarization structure, in this section we show some examples of the different behaviors found.

We chose these simple examples for illustrating the effect of non-linearity, one changing the growth power of the azimuthal phase without changing the total modulation and the other setting up a non-linear modulation that leaves null the net topological charge.

### A. Polynomial growth

We have simulated a plate defined by the non linear function $\Phi(\theta) = q(2\pi)^{(1-p)}\theta^p$. The multiplicative constant $(2\pi)^{(1-p)}$ is due to the continuity condition: $\Phi(2\pi) = q2\pi$, meaning that the total azimuthal variation is $q$ times $2\pi$, without discontinuous steps in $\Phi$ after a $2\pi$ period in $\theta$. Figure 1 shows some examples of the simulated argument function of these plates ($2\Phi(\theta)$) for different powers $p$ and values of $q$. The total azimuthal variation of the argument function is given by $2q$ times $2\pi$, which defines the topological charge of the created beams, as will be seen soon. These beams illustrate in a simple way the effect of breaking linearity in the q-plate element, both in near and far field propagation.

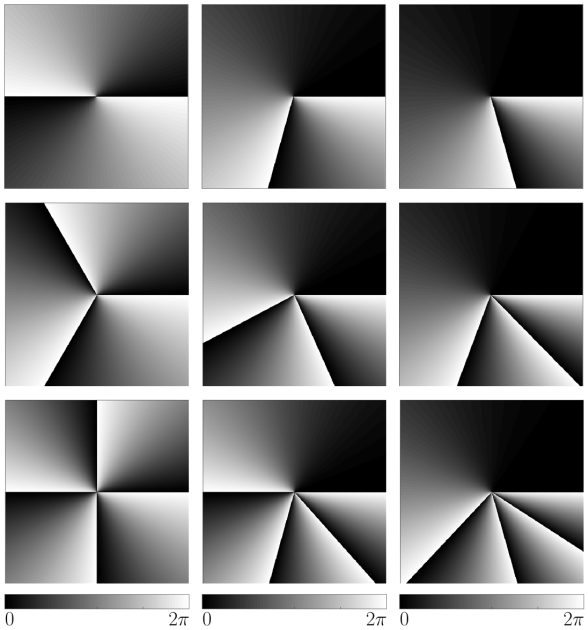


FIG. 1: Argument phase function of the Gq-plates determined by a polynomial growth in $\theta$. The first, second and third columns show the cases for powers $p = 1$, $p = 2$ and $p = 3$, respectively; while first, second and third rows show the cases for topological charges $q = 1$, $q = 3/2$ and $q = 2$, respectively.

We studied how these Gq-plates affect an input beam with uniform phase and intensity within a circular profile (top-hat beam), simulating both the obtained field just after passing through the plate and that obtained in the far field approximation, i.e., the Fraunhofer diffraction of the former. For a vector field, this is performed simply by computing the Fourier transform of each of the $\hat{x}$ and $\hat{y}$ components of the field [20],

$$\begin{aligned} \mathcal{F}\{\mathbf{E}(x,y)\} &= \tilde{\mathbf{E}}(u,v) \\ &= \begin{pmatrix} \tilde{E}_s(u,v) \\ \tilde{E}_p(u,v) \end{pmatrix} \\ &= \begin{pmatrix} \mathcal{F}\{E_s(x,y)\} \\ \mathcal{F}\{E_p(x,y)\} \end{pmatrix}. \end{aligned} \qquad (3)$$

This is implemented numerically by means of the two dimensional discrete Fourier transform of an N × N matrix, where each element is the corresponding value of the electric field $\mathbf{E}(x,y)$ after passing through the Gq-plate.

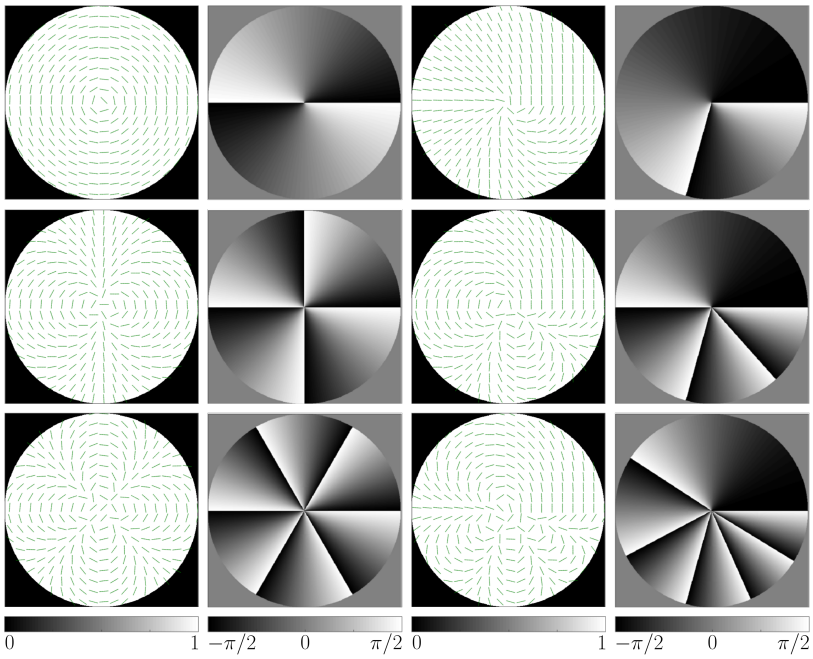


FIG. 2: (Color online) Polarization ellipses and its azimuth resulting from input vertical polarization for polynomial Gq-plates. First and third columns show intensity and polarization ellipses for $p = 1$ and $p = 2$, respectively. Second and fourth columns show polarization azimuth for $p = 1$ and $p = 2$, respectively. First, second and third rows show cases with topological charges $q = 1/2$, $q = 1$ and $q = 3/2$, respectively. The output consists on vector beams in which the azimuth grows accordingly to the power $p$.

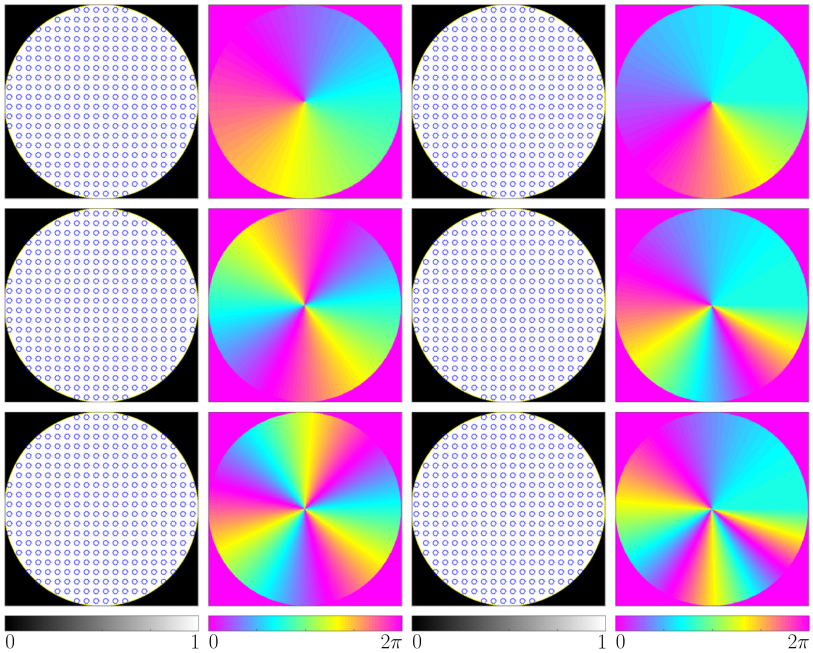


FIG. 3: (Color online) Polarization ellipses and phase distributions resulting from input left circular polarization for polynomial Gq-plates. First and third columns show intensity and polarization ellipses for $p = 1$ and $p = 2$, respectively. Second and fourth columns show phase for $p = 1$ and $p = 2$, respectively. First, second and third rows show cases with topological charges $q = 1/2$, $q = 1$ and $q = 3/2$, respectively. The output consists on uniformly right circular polarized beams in which phase grows accordingly to the power $p$.

Figure 2 shows the intensity and polarization distribution, as well as the azimuth of the polarization ellipses, at the output plane of the Gq-plate (the last one is represented with a gray scale from $-\pi/2$ to $\pi/2$), for powers $p = 1$ and $p = 2$, and different values of $q$, when the input beam is linearly polarized in the vertical direction. The azimuth of the polarization ellipses is obtained by computing the phase of the complex Stokes field $S_{12}(x, y) = S_1(x, y) + iS_2(x, y)$, where $S_i(x, y)$ are the Stokes parameters of the electric field [21].

In the case when $p = 1$ (linear q-plate) and $q = 1/2$ it is obtained an azimuthally polarized vector beam, whose topological charge is determined by the number of times that the polarization vector gives a complete turn around the beam axis [16] (in this case $2q = 1$). When increasing the power to $p = 2$ the topological charge does not change, while the cylindrical symmetry is lost, since the azimuth grows quadratically with $\theta$. Same behavior is seen for higher topological charges.

In Fig. 3 it is analyzed the behavior of these elements when they are illuminated with circularly polarized light. In this case the polarization ellipse fields and the beam phase distributions are shown. We choose (from now on) to represent these magnitudes because, as a general fact for q-plates, when input polarization is linear, the modulation occurs in the polarization field, but when input polarization is circular, it occurs in the phase of the field, while the polarization remains uniform, with opposite sense of rotation due to the STOC phenomenon.

As it was previously said, for input left circular polarization it is observed the STOC phenomenon, giving place to an output uniform right circularly polarized beam, carrying OAM with topological charge $l = 2q$. This is seen in the $2\pi$ turn of the beam phase around the propagation axis. The way phase grows depends on the power $p$.

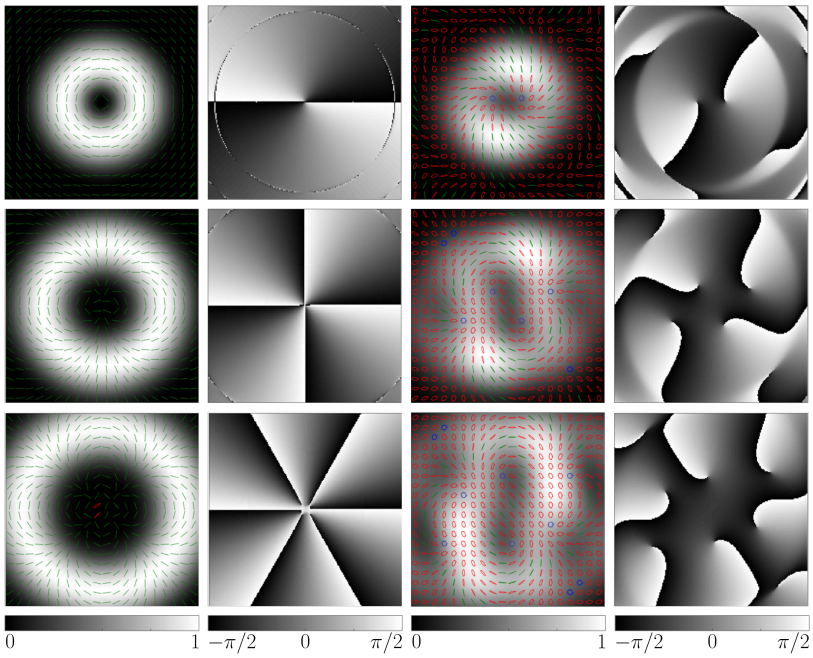


FIG. 4: (Color online) Polarization ellipses and its azimuth resulting from input vertical polarization for polynomial Gq-plates, in the far field regime. The first and third columns show the intensity distribution and polarization structure for $p = 1$ and $p = 2$, respectively. The second and fourth columns show the azimuth of the polarization ellipses for $p = 1$ and $p = 2$, respectively. The first, second and third rows show the cases for $q = 1/2$, $q = 1$ and $q = 3/2$, respectively.

An interesting effect arises when the Fraunhofer diffraction patterns of these beams are calculated. Figure

4 shows the result from propagating the output beams obtained when impinging with linear vertical polarization (Fig. 2). Both, the polarization ellipses superposed to the intensity distribution and the azimuth of the ellipses are represented. In order to plot the polarization ellipses we used a color code based on the respective form factor $f = b/a$, the ratio between the minor $b$ and mayor $a$ axis of the ellipse, whose sign depends on the vector sense of rotation (negative for right-handed, and positive for left-handed). There is a neighborhood around $f = 0$ for which we considered polarization to be linear (green), and a neighborhood around $f = \pm 1$ for which we considered polarization to be circular (blue), in any other case the polarization is elliptical (red).

For linear q-plates ($p = 1$) the polarization field in the Fraunhofer regime is the same as in the q-plate plane, with a "donut" intensity distribution, due to the central polarization vortex [11]. Conversely, the beams obtained from non linear Gq-plates do not preserve their polarization fields, non-linearities break the cylindrical symmetry of the SoP and intensity distributions. It can be seen that instead of showing a central singularity with topological charge $2q$, they show $4q$ isolated singularities each one with topological charge $1/2$, adding up to a total charge of $2q$. Furthermore, the nature of these singularities differs from the original dark singularity. In Fig. 5 this fact is shown in detail for one of these singularities. It can be seen that the azimuth is not defined in these points although the form factor is, and is maximum (left circular polarization). These singularities are generally known as C-points: isolated points of circular polarization around which polarization azimuth rotates in $m2\pi$. The topological charge in these cases is $m = 1/2$.

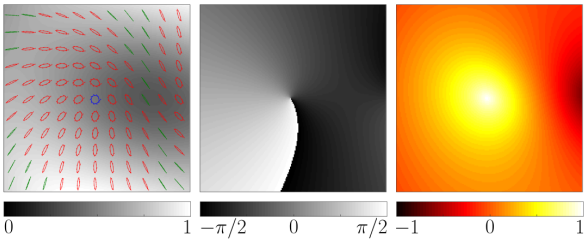


FIG. 5: (Color online) Zoom of one of the polarization singularities obtained in the far field for a polynomial Gq-plate with $q = 1/2$ and $p = 2$, when input polarization is vertical. Left: intensity and polarization ellipses. Center: azimuth of the polarization ellipses. Right: form factor of the polarization ellipses.

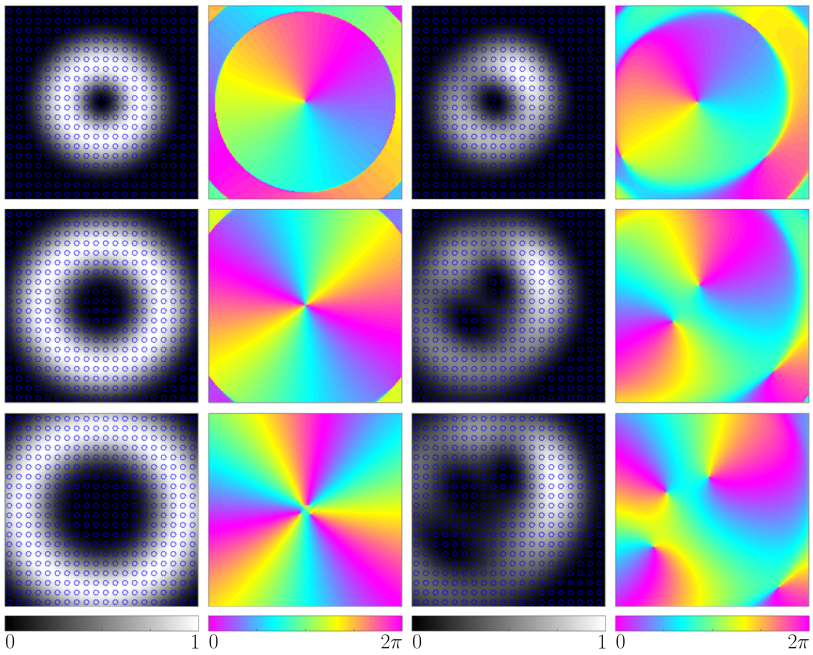


FIG. 6: (Color online) Polarization ellipses and phase distribution resulting from an input beam with left circular polarization for polynomial Gq-plates, in the far field regime. The first and third columns show the intensity distribution and polarization structure for $p = 1$ and $p = 2$, respectively. Polarization is in every case uniform right circular. The second and fourth columns show the phase of the field for $p = 1$ and $p = 2$, respectively. The first, second and third rows show the cases for $q = 1/2$, $q = 1$ and $q = 3/2$, respectively.

Figure 6 shows the Fraunhofer diffraction of the beams obtained when impinging onto the Gq-plates with left circularly polarized light. In this case, for a linear q-plate, the phase and polarization distributions are identical to those seen in the q-plate plane, with a central singularity (phase vortex) with topological charge $2q$, due to the creation of OAM. In the non linear case, $2q$ isolated vortexes with topological charge 1 appear, occupying the same position as half of the C-points obtained in the case of linearly polarized light (Fig. 4). If impinging with right circularly polarized light (not shown), there would be another $2q$ vortexes, located according to the other half of the C-points. These non uniform intensity and phase gradients may give place to novel optical force fields applicable to optical trapping and micromanipulation [22].

This singularity splitting can be explained in terms of the far field (Fraunhofer) diffraction phenomenon. Fraunhofer field coincides with the Fourier transform of the field at the Gq-plate plane, which (for a function $g(r,\theta)$ separable in polar coordinates) can be written in terms of an infinite sum of weighted Hankel transforms [23],

$$\mathcal{F}\{g(r,\theta)\} = \sum_{k=-\infty}^{\infty} c_k (-i)^k e^{ik\phi} \mathcal{H}_k\{g_R(r)\}, \quad (4)$$

where

$$c_k = \frac{1}{2\pi}\int_0^{2\pi} g_\Theta(\theta) e^{-ik\theta} d\theta \quad (5)$$

and $\mathcal{H}_k$ is the Hankel transform operator of order $k$,

$$\mathcal{H}_k\{g_R(r)\} = 2\pi \int_0^{\infty} r g_R(r) J_k(2\pi r\rho) dr, \quad (6)$$

being $J_k$ the $k$th-order Bessel function of the first kind, and $g(r,\theta) = g_R(r) g_\Theta(\theta)$.

With this in mind we can take as an example the cases shown in Fig. 2 for $q = 1/2$ and calculate the weight distributions in each case. In the linear case ($p = 1$), when input light is vertically polarized, the electric field after the q-plate is obtained from Eq. 2,

$$\begin{aligned}\mathbf{E}_o(r,\theta) &= M_\Phi(r,\theta)\mathbf{E}_i(r,\theta) \\ &= \begin{pmatrix} \cos(\theta) & \sin(\theta) \\ \sin(\theta) & -\cos(\theta) \end{pmatrix} \begin{pmatrix} 0 \\ E_i \end{pmatrix} \\ &= E_i \begin{pmatrix} \sin(\theta) \\ -\cos(\theta) \end{pmatrix} \\ &= \begin{pmatrix} E_s(r,\theta) \\ E_p(r,\theta) \end{pmatrix},\end{aligned} \quad (7)$$

while in the non-linear case with $p = 2$,

$$\mathbf{E}_o(r,\theta) = \begin{pmatrix} E_s(r,\theta) \\ E_p(r,\theta) \end{pmatrix} = E_i \begin{pmatrix} \sin(\frac{1}{2\pi}\theta^2) \\ -\cos(\frac{1}{2\pi}\theta^2) \end{pmatrix}. \quad (8)$$

We computed the Fourier transform of these fields according to Eqs. 3 and 4, to obtain the respective weights $C_k^2 = c_{s_k}^2 + c_{p_k}^2$, where $c_s$ and $c_p$ stand for the weights of the Fourier transforms of the fields $E_s(r,\theta)$ and $E_p(r,\theta)$ respectively. Results are shown in Fig. 7.

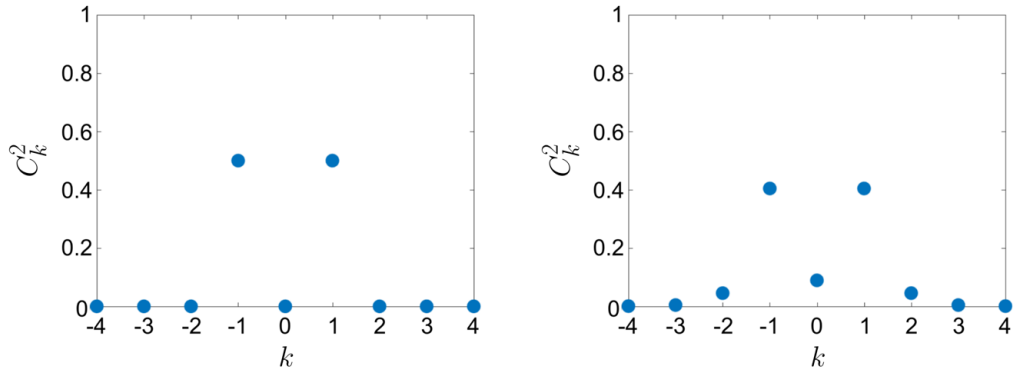


FIG. 7: Normalized weights $C_k^2 = c_{s_k}^2 + c_{p_k}^2$ of the terms in the Fourier transforms of the fields created with polynomial Gq-plates with $q = 1/2$ when input beam is vertically polarized. Left: linear case ($p = 1$). Right: non-linear case ($p = 2$).

In the case $p = 1$ the only non-zero terms are $k = 1$ and $k = -1$, both terms and the sum of them are shown in Fig. 8. This, as expected, is identical to the field shown in Fig.4. On the other hand, in the case with $p = 2$, while terms $k = 1$ and $k = -1$ remain the most significant, other terms arise, in particular that with $k = 0$. This term contributes with a Bessel function $J_0$, giving non-zero intensity at the propagation axis, and hence destroying the dark singularity, as shown in Fig. 9. Since at the beam axis the only non-zero term is the $k = 0$, the polarization there is linear at $-55°$. In the outer region, the predominant terms $k = 1$ and $k = -1$ create a cylindrically polarized vector beam. The continuous transition between the SoP at the center and in the outer region, and the phase difference between these terms due to the factor $(-i)^k$ in Eq. 4, force the apparition of two C-points. It is worth to mention why field in Fig. 9b differs from that in Fig. 8c. Even though they are both sums of terms with $k = -1$ and $k = 1$ with equal weighting, in the non-linear case the Fourier decomposition of vertical component $E_p(r, \theta)$ gives higher weight to these terms respect to other $k$ values than the decomposition for the horizontal component $E_s(r, \theta)$. This results in higher intensity for the vertically polarized light when terms with $k = -1$ and $k = 1$ are added, hence breaking the cylindrical symmetry.

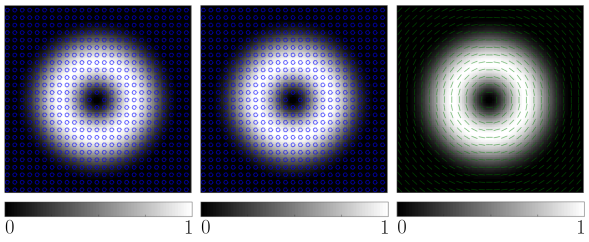


FIG. 8: (Color online) Intensity and polarization patterns of Fourier transform terms of a field created with a polynomial Gq-plate with $q = 1/2$ and $p = 1$, for vertically polarized input light. Left: term with $k = -1$. Center: term with $k = 1$. Right: sum of both terms.

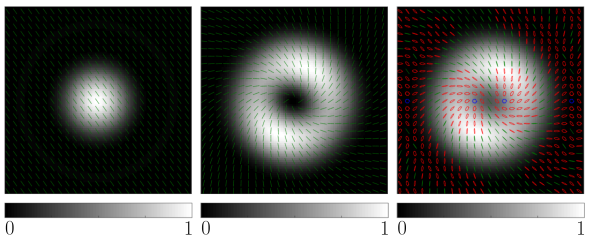


FIG. 9: (Color online) Intensity and polarization patterns of Fourier transform terms of a field created with a polynomial Gq-plate with $q = 1/2$ and $p = 2$, for vertically polarized input light. Left: term with $k = 0$. Center: sum of terms with $k = -1$ and $k = 1$. Right: sum of terms with $k = -1$, $k = 0$ and $k = 1$.

It is interesting to analyze how these fields evolve from their pass through the Gq-plate to the far field regime, and how is the transition between the central singularity and the multiple isolated singularities. For that purpose we have simulated the device depicted in Fig. 10. We have added a quadratic phase to the field, representing the effect of a lens, and numerically calculated the Fresnel diffraction integral for transverse planes at different distances $z$, from the lens plane $z = 0$ to the focus $z = \mathbf{f}$. The field distribution at the focal plane is equal to that obtained by directly Fourier transforming (Fraunhofer diffraction). Intermediate planes show the beam polarization structure in the near field regime.

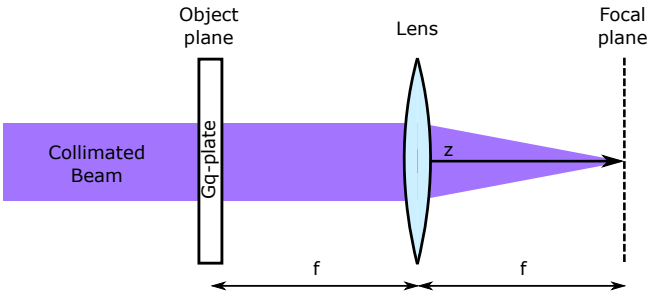


FIG. 10: (Color online) Scheme of the optical device used for computing the beam evolution as it propagates from the Gq-plate to the far field regime.

Figure 11 shows some of the propagated fields for the case $q = 1/2$, $p = 2$, when the input beam is vertically polarized. A short movie showing the complete evolution is included in the Supplemental Material [24]. For distances close to the lens plane, i.e., when $z < \mathbf{f} - \mathbf{f}/2$, the intensity of the beam remains approximately constant, and the polarization structure is the same as in the Gq-plate plane, with a central singularity, this is in agreement with the results reported in reference [16]. For $z = \mathbf{f} - \mathbf{f}/8$ the polarization field begins to distort, showing regions in which polarization is elliptical. Further on, e.g., when $z = \mathbf{f} - \mathbf{f}/32$, two critical points of the form factor clearly appear, in the center of the beam, and the central singularity is divided in two, although most of the polarization structure remains similar to that at $z = 0$. Finally at the focal plane the polarization structure is totally distorted, showing elliptic polarization around two C-points with topological charge 1/2, and no central point with null intensity. It is remarkable that the SoP, which in principle does not show any symmetry, in the far field regime gains symmetry with respect to the transformation that rotates the beam $\pi$ radians around its axis and inverts the rotation of the polarization vector. When input polarization is left (right) circular, polarization turns right (left) circular and remains uniform during propagation. Phase distribution remains unmodified for distances close to the lens plane, and then distorts into the singularities discussed earlier.

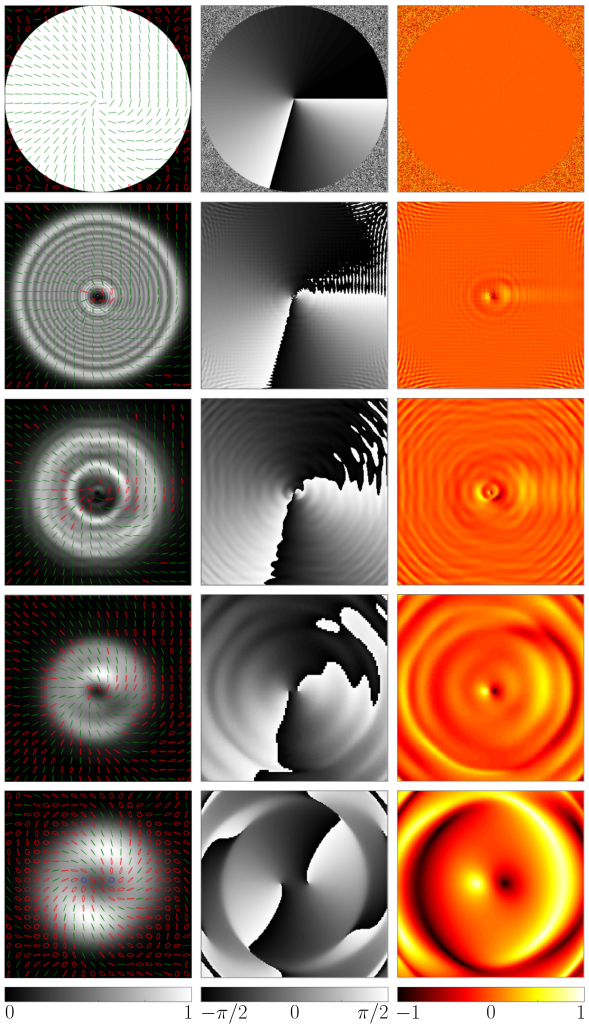


FIG. 11: (Color online) Fresnel diffraction pattern at different planes resulting from a polynomial Gq-plate with $q = 1/2$ and $p = 2$, when the input light is vertically polarized. The intensity distribution superposed to the polarization ellipses are shown in the first column. The azimuth and form factor are depicted in the second and third column respectively. Rows show the evolution in the $z$ coordinate, for $z = 0$, $z = \mathbf{f} - \mathbf{f}/2$, $z = \mathbf{f} - \mathbf{f}/8$, $z = \mathbf{f} - \mathbf{f}/32$ and $z = \mathbf{f}$, respectively.

### B. Sinusoidal variation

Another possibility is that of designing an element that modulates the electric field without adding any net topological charge, e.g., a Gq-plate defined by an oscillating function in $\theta$. That is the case for the function $\Phi(\theta) = -(\pi/2)(\cos(q\theta) - 1)$, where $2\Phi$ (Eq. 2 matrix argument) oscillates between 0 and $2\pi$, being $q$ the number of periods for $\theta \in [0, 2\pi]$. Figure 12 shows some examples of this function for different values of $q$.

Figure 13 shows the results obtained from some of these Gq-plates when vertically and left circularly polarized beams are used to illuminate the element. For vertically polarized input, it is achieved an output with uniform phase distribution and a polarization whose azimuth oscillates, while for circularly polarized input an oscillating phase distribution with uniform polarization is obtained. Again, as discussed in the previous section, at the exit of the Gq-plate the function $\Phi$ defines the polarization structure when impinging with linear polarization and the phase structure when impinging with circular polarization. Novel effects occur in the far field beyond the Gq-plate, as shown in Fig. 14. There it is shown the Fraunhofer diffraction fields obtained after impinging onto this kind of Gq-plate with vertically polarized light. Yellow contours delimit the minimum intensity areas, defined as the regions with less than 0.5% of maximum intensity.

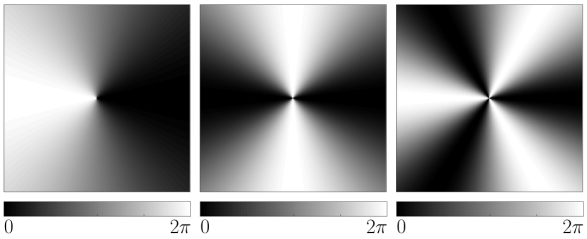


FIG. 12: Argument function ($2\Phi(r, \theta)$) for sinusoidal Gq-plates with $q = 1$, $q = 2$ and $q = 3$, respectively.

It can be observed an interesting behavior that depends on the parity of $q$. For odd $q$ values, the diffraction pattern shows several intensity minima, which match with corresponding saddle points in the form factor, keeping the azimuth of the polarization ellipses according to the input beam (except for 90° rotations). On the other hand, for even $q$ values, form factor remains uniformly zero (linear polarization), while $2q$ dark azimuth singularities arise, which match with corresponding $2q$ intensity minima, distributed geometrically around the beam axis. These singularities have alternate $\pm 1$ topological charges, adding up 0. Topological charge is measured as the times that the azimuth completes a $2\pi$ rotation along a closed path around the singularity, and the sing is provided by the sense of rotation, positive charge singularities are known as flowers, while negative charge singularities are known as webs [21].

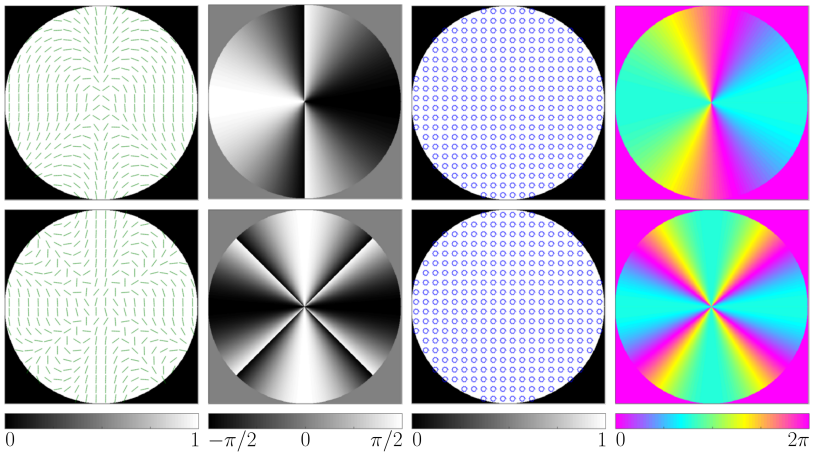


FIG. 13: (Color online) Results provided by sinusoidal Gq-plates with $q = 1$ (first row) and $q = 2$ (second row). First column shows intensity and polarization distribution for vertical input polarization and second column shows its respective azimuth. Third column shows intensity and polarization distribution for left circular input polarization and fourth column shows its respective phase.

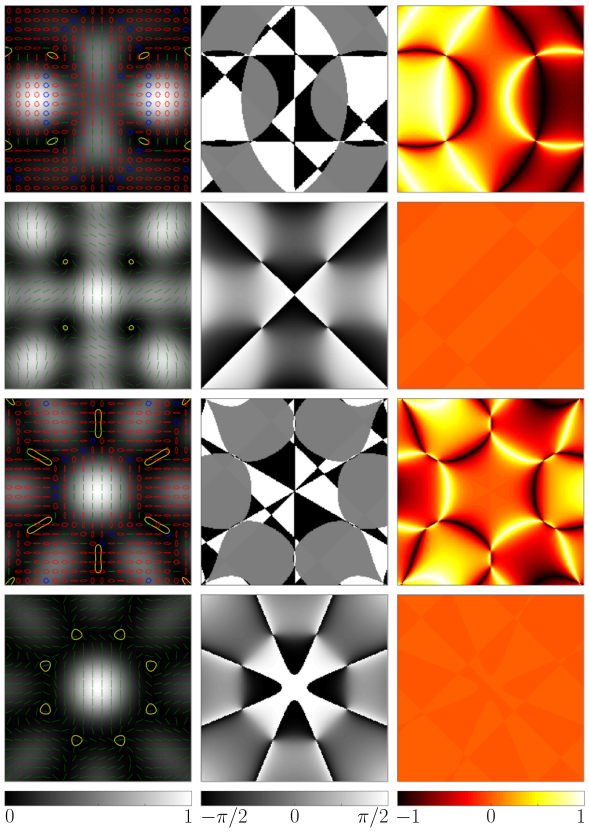


FIG. 14: (Color online) Results for sinusoidal Gq-plates in the far field regime when input polarization is vertical. The first column shows polarization and intensity distribution, second column shows azimuth, and third column shows form factor. Rows show the cases for $q = 1$, $q = 2$, $q = 3$ and $q = 4$, respectively. Yellow lines demarcate minimum intensity areas.

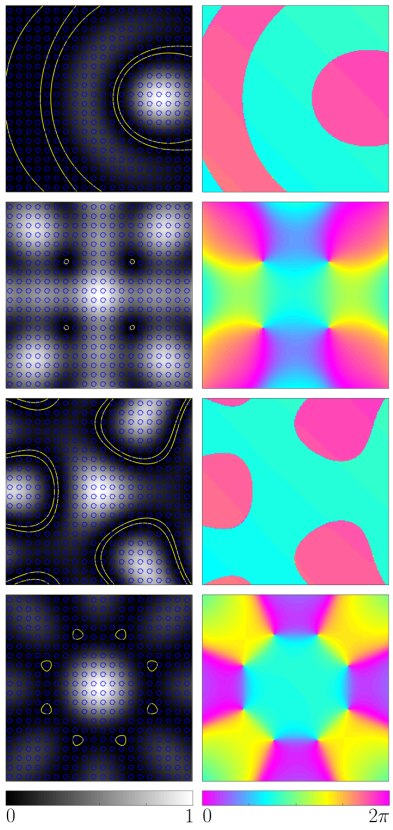


FIG. 15: (Color online) Results for sinusoidal Gq-plates in the far field regime when input polarization is left circular. First column shows intensity and polarization distribution, while second column shows phase distribution. Rows show the cases for $q = 1$, $q = 2$, $q = 3$ and $q = 4$, respectively. Yellow lines demarcate minimum intensity areas.

This can be explained as well in terms of the Fourier transform decomposition of Eq. 4 discussed earlier. For instance, when input light is vertically polarized, the electric field at the exit of the Gq-plate is

$$\mathbf{E}_o(r,\theta) = \begin{pmatrix} E_s(r,\theta) \\ E_p(r,\theta) \end{pmatrix} = E_i \begin{pmatrix} \sin(-\pi(\cos(q\theta)-1)) \\ -\cos(-\pi(\cos(q\theta)-1)) \end{pmatrix}. \tag{9}$$

If we look at the $c_k$ values of the Fourier transform of this field, it is found that for odd $q$ values, $E_s$ shows in its expansion only terms with odd $k$ value, while $E_p$ shows only even valued terms. Since all $c_k$ values are real in this case, it means that the horizontal component of the electric field has a phase factor $(-i)^k = \pm i$, while the vertical component has a phase factor $(-i)^k = \pm 1$. Then, the phase difference between these components has to be $\pm\pi/2$, giving polarization ellipses vertically or horizontally oriented, with a form factor depending on the amplitude ratio. On the other hand, for even $q$ values, Fourier expansion of both components of the electric field shows only terms with even $k$ values, so phase difference between them must be 0 or $\pm\pi$, giving now linear polarization with azimuth depending on the amplitude ratio.

Similar distinction occurs when the polarization of the input beam is left circular, as shown in Fig. 15. For odd $q$ values, there are no isolated singularities, but minima valleys which set a $\pi$ step in the beam phase. Regarding Fig. 14 it can be seen that these minima valleys match left circularly polarized regions resulting from vertically polarized input. A vertically polarized beam can be described as the balanced superposition of left and right circularly polarized beams, and after passing through the Gq-plate, left circular polarization turns right, and vice versa. Then, its reasonable that when input light is left circularly polarized, regions of the output beam corresponding to left circular maxima show no intensity. On the other hand, for even $q$ values there are $2q$ phase vortexes carrying alternate topological charges (OAM) of $\pm 1$, matching respective intensity isolated minima. Again, the total topological charge adds up to 0. Comparing with the case with linearly polarized input, intensity distributions are the same, changing polarization vortexes into phase vortexes now. This is consistent, since sinusoidal Gq-plates with even $q$ values seems to modulate left and right circularly polarized light in the same way. This kind of distribution of optical vortexes with alternate charges around the beam axis may have potential application in optical trapping and micromanipulation [25].

## III. PROPOSED DEVICE TO MIMIC A GENERALIZED Q-PLATE

Beyond studying the new effects achieved by these novel devices it is essential to provide an effective and efficient method for experimental implementation, which is vital for exploring new applications.

Q-plates are typically inhomogeneous and anisotropic devices where effects like STOC are related to the Pancharatnam-Berry phase [26]. Here instead we propose a compact device that makes use of the propagation phase modulation provided by a phase only SLM for emulating the effect of the generalized q-plates described above. The device is designed for modulating independently the phase of the orthogonal components of an input electric field, using a commercially available parallel aligned reflective liquid crystal on silicon (PA-LCoS) display. This kind of display introduces a programmable phase modulation to one linear component of the field (let us suppose that the director of the LC molecules is horizontally oriented). The proposed setup is sketched in Fig. 16 and is based on a similar architecture used to encode q-plates by I. Moreno et al [16]. There, the authors employ a parallel aligned transmission display, which is an unusual device.

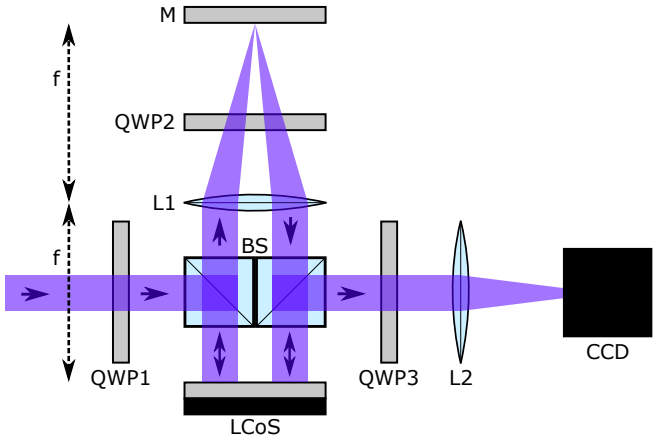


FIG. 16: (Color online) Experimental compact device proposed for emulating generalized q-plates using a reflective PA-LCoS.

Let us describe how to get the desired modulation with this setup. The incident collimated beam passes through a first quarter wave plate (QWP1) oriented at 45° and is reflected by means of a first beam-splitter (BS) onto one half of the LCoS, where a phase of $\psi = 2\Phi(r,\theta)$ is added to the horizontal component of the electric field. Then the beam propagates along a 4f system, where a quarter wave plate (QWP2) oriented at 45° respect to the LC director, rotates the polarization vector in $-\pi/2$, due to the double passage caused by reflecting the beam with a mirror (M) located at the focus of L1. On the other half of the LCoS, a phase $-\psi = -2\Phi(r,\theta)$ is added to the remaining orthogonal component, and by means of a second beam-splitter, the reflected modulated beam goes through a third quarter wave plate (QWP3) oriented at $-45°$, and towards a CCD. Lens L2 is useful for measuring the output beam at different propagation distances, between near and far field regimes, it can be removed for observing directly the intensity obtained at the exit of the device.

Although this device is not related directly to Pancharatnam-Berry phase, its matrix representation coincides with that of the Gq-plate (Eq. 2), up to a global phase factor, then emulating all the expected behaviors. On the other hand, since it is possible to program it pixel by pixel, it allows to make modifications at video rates, adding flexibility in the design of the mimicked plates, and allowing an efficient and dynamic testing of these devices without requiring its fabrication.

## IV. CONCLUSIONS

We simulated generalized q-plates (Gq-plates) which modulate the incident beam with non-linear functions of the azimuthal variable, and studied their effects on uniform linearly and circularly polarized beams. Furthermore, we proposed an experimental device capable of implementing these novel devices in a dynamic and efficient way.

In the near field approximation it is found that for linearly polarized input, the output polarization structure is given by the argument function of the Gq-plate, showing a central singularity, characteristic of conventional vector beams, while for circularly polarized input the output phase structure is the one modulated, giving place to the generation of OAM and the inversion of the polarization sense (STOC phenomenon).

In the far field regime, it is found that when losing linearity in the azimuthal variable, the conventional central singularity divides into several singularities of minimum topological charge. In the cases where the input light is linearly polarized, the output beam can exhibit, either C-points with topological charge $\pm 1/2$, as well as other types of critical points of the form factor, or dark polarization singularities (flowers/webs). Circularly polarized input beams, result in the appearance of phase vortexes, carrying OAM with topological charge $\pm 1$. The intensity profiles and singularity distributions in each case depends on the particular chosen function $\Phi$, giving the chance to model distributions of any optical singularity known. these results were analyzed and discussed in terms of Fourier decomposition for separable functions in cylindrical coordinates.

Since the list of q-plate based applications is extensive and still in growth [26], we think Gq-plates based on arbitrary functions, together with capability of representing these functions by means of an experimental device based on a PA-LCoS, which gives flexibility to the creation and manipulation of novel vector and vortex beams, opens a wide range of possibilities for experimental research of new distributions of intensity, phase and polarization, as well as singularities or critical points of different kind, which are expected to have potential applications, e.g. in the field of singular optics and optical tweezers.

## ACKNOWLEDGMENTS

This work was supported by UBACyT Grant No. 20020170100564BA, and ANPCYT Grant No. PICT 2014/2432. M.V. holds a CONICET Fellowship.

[1] Q. Zhan, *Vectorial Optical Fields: Fundamentals and Applications* (World Scientific Publishing, 5 Toh Tuck Link, Singapore, 2013).
[2] Q. Zhan, Adv. Opt. Photon. **1**, 1 (2009).
[3] S. Quabis, R. Dorn, M. Eberler, O. Glöckl, and G. Leuchs, Opt. Commun. **179**, 1 (2000).
[4] W. Cheng, J. W. Haus, and Q. Zhan, Opt. Express **17**, 17829 (2009).
[5] M. Woerdemann, C. Alpmann, M. Esseling, and D. C., Laser Photonics Rev. **7**, 839–854 (2013).
[6] Q. Zhan, Opt. Express **12**, 3377 (2004).
[7] H. Kawauchi, K. Yonezawa, Y. Kozawa, and S. Sato, Opt. Lett. **32**, 1839–1841 (2007).
[8] Y. Zhao, Q. Zhan, Y. Zhang, and Y. Li, Opt. Letters **30**, 848–850 (2005).
[9] M. Duocastella and C. Arnold, Laser Photonics Rev. **6**, 607–621 (2012).
[10] C. Gabriel, A. Aiello, W. Zhong, T. Euser, N. Joly, P. Banzer, M. Förtsch, D. Elser, U. Andersen, C. Marquardt, P. Russell, and G. Leuchs, Phys. Rev. Lett. **106**, 060502 (2011).
[11] F. Cardano, E. Karimi, S. Slussarenko, L. Marrucci, C. de Lisio, and E. Santamato, Appl. Opt. **51**, C1 (2012).
[12] L. Marrucci, C. Manzo, and D. Paparo, Appl. Phys. Lett. **88**, 221102 (2006).
[13] L. Marrucci, C. Manzo, and D. Paparo, Phys. Rev. Lett. **96**, 163905 (2006).
[14] L. Marrucci, E. Karimi, S. Slussarenko, B. Piccirillo, E. Santamato, E. Nagali, and F. Sciarrino, J. Opt. **13**, 064001 (2011).
[15] A. Hermerschmidt, S. Osten, S. Krüger, and T. Blümel, Proc. SPIE **6584**, 65840E (2007).
[16] I. Moreno, M. M. Sanchez-Lopez, K. Badham, J. A. Davis, and D. M. Cottrell, Opt. Lett. **41**, 1305 (2016).
[17] W. Ji, C. Lee, P. Chen, W. Hu, Y. Ming, L. Zhang, T. Lin, V. Chigrinov, and Y. Lu, Sci. Rep. **6**, 25528 (2016).
[18] J. E. Holland, I. Moreno, J. A. Davis, M. M. Sánchez-López, and D. M. Cottrell, Appl. Opt. **57**, 1005 (2018).
[19] M. Rafayelyan and E. Brasselet, Opt. Lett. **42**, 1966 (2017).
[20] I. Moreno, M. Yzuel, J. Campos, and A. Vargas, J. Mod. Opt. **51**, 2031 (2004).
[21] I. Freund, M. Soskin, and A. I. Mokhun, Opt. Commun. **208**, 223 (2002).
[22] M. Padgett and R. Bowman, Nat. Photonics **5**, 343–348 (2011).
[23] J. W. Goodman, *Introduction to Fourier Optics* (McGraw-Hill, 1996).
[24] See Supplemental Material at [URL] for a short movie showing the complete evolution of a beam propagating from the Gq-plate plane to the far field regime.

[25] M. Gecevicius, R. Drevinskas, M. Beresna, and P. Kazansky, Appl. Phys. Lett. **104**, 231110 (2014).

[26] A. Rubano, F. Cardano, B. Piccirillo, and L. Marrucci, J. Opt. Soc. Am. B **36**, D70 (2019).